Viscoelastic Relaxation in the Membrane of the Auditory Outer Hair Cell

David Ehrenstein and K. H. Iwasa
Biophysics Section, Laboratory of Cellular Biology, National Institute on Deafness and Other Communication Disorders, National Institutes of Health, Bethesda, Maryland 20892-0922 USA

ABSTRACT The outer hair cell (OHC) in the mammalian ear has a unique membrane potential-dependent motility, which is considered to be important for frequency discrimination (tuning). The OHC motile mechanism is located at the cell membrane and is strongly influenced by its passive mechanical properties. To study the viscoelastic properties of OHCs, we exposed cells to a hypoosmotic solution for varying durations and then punctured them, to immediately release the osmotic stress. Using video records of the cells, we determined both the imposed strain and the strain after puncturing, when stress was reset to zero. The strain data were described by a simple rheological model consisting of two springs and a dashpot, and the fit to this model gave a time constant of 40 ± 19 s for the relaxation (reduction) of tension during prolonged strain. For time scales much shorter or longer than this, we would expect essentially elastic behavior. This relaxation process affects the membrane tension of the cell, and because it has been shown that membrane tension has a modulatory role in the OHC's motility, this relaxation process could be part of an adaptation mechanism, with which the motility system of the OHC can adjust to changing conditions and maintain optimum membrane tension.

INTRODUCTION

The outer hair cell (OHC) is one of the mechanoreceptor cells in the mammalian cochlea. Because the OHC has voltage-dependent motility (Brownell et al., 1985; Ashmore, 1987; Santos-Sacchi and Dilger, 1988; Iwasa and Kachar, 1989), the receptor potential caused by mechanical oscillations in the cochlea produces cell movement, which can modify the mechanical oscillations. It has been hypothesized that this feedback mechanism plays a significant role in the exquisite sensitivity and frequency discrimination (tuning) in mammalian hearing (Lieberman and Dodds, 1984; De Boer, 1991).

The mechanism for this membrane potential-dependent motility is unique in that the motor is neither ATP-dependent (Kachar et al., 1986; Holley and Ashmore, 1988) nor Ca^{2+}-sensitive (Holley and Ashmore, 1988; Iwasa et al., 1995). The motile mechanism is localized in the lateral plasma membrane (Dallos et al., 1991; Kalinec et al., 1992; Huang and Santos-Sacchi, 1993) and is believed to be based on membrane proteins that undergo conformational changes in response to membrane potential (Dallos et al., 1993; Iwasa, 1993; Santos-Sacchi, 1993; Ashmore, 1994; Iwasa, 1994). The conformational changes of these motile units may be characterized by monitoring the cell's membrane capacitance, which depends on both membrane potential and membrane tension (Iwasa, 1993; Gale and Ashmore, 1995; Kakehata and Santos-Sacchi, 1995). The potential and tension dependence of capacitance is a manifestation of the direct electromechanical coupling in the lateral plasma membrane of the OHC, and it allows evaluation of the membrane area changes of the motor units (Iwasa, 1993, 1994, 1996). The membrane tension depends on both motor elements and passive mechanical elements of the cell, so passive mechanical properties are important for the OHC's function.

There are few cytoskeletal structures in the cell body connected to the membrane except for the ones underlying the membrane. Thus, it is reasonable to assume that the mechanical properties of the cell can be described by a thin layer including the plasma membrane and the cytoskeleton just below it (Iwasa et al., 1991; Iwasa and Chadwick, 1992). The regular cylindrical shape of the cell simplifies the description of stress-strain relationships (Iwasa and Chadwick, 1992; Iwasa, 1993, 1994; Tolomeo and Steele, 1995).

The purpose of this study is to clarify the limits of the purely elastic treatment of the OHC that has been used in modeling. We found that the cell membrane is viscoelastic (Evans and Skalak, 1980; Poznanski et al., 1992; Sung and Chien, 1992; Hochmuth, 1993), although the elastic approximation is valid for time scales much longer or shorter than the time constant for viscoelastic relaxation. We determined the time dependence of membrane tension in response to an applied strain by measuring strain immediately after stress was released. This "release strain" was a probe of the stress that existed before the release. We used hypoosmotic perfusion as the means of applying measurable strains to the cell, and puncturing it was our method of releasing osmotic stress. We found the characteristic time for viscoelastic changes in the cell membrane to be about 40 s.

Received for publication 17 October 1995 and in final form 2 May 1996.
Address reprint requests to Dr. David Ehrenstein, National Institutes of Health, Bldg. 9, Rm. 1E114, MSC 0922, Bethesda, MD 20892-0922. Tel.: 301-496-7232; Fax: 301-480-0827; E-mail: david-e@nih.gov.

0006-3495/96/08/1087/08 $2.00

MATERIALS AND METHODS

Cell preparation

Isolated OHCs were obtained from guinea pig cochleas as described earlier (Iwasa, 1993). The OHCs were mechanically dissociated from dissected

organ of Corti without enzyme treatments. Cells with high optical contrast and of clean cylindrical shape were selected for the experiment. The OHCs used ranged from 20 to 70 μm in length in the standard saline.

Hypoosmotic perfusion

Stress was applied to cells by hypoosmotic perfusion. The perfusion setup included a pipette (mouth diameter about 5 μm) filled with a hypoosmotic medium connected with an air pump (pressure from 1 to 2 kPa) through a solenoid valve. The standard bathing medium consisted of NaCl (140 mM), KCl (5 mM), $MgCl_2$ (2 mM), $CaCl_2$ (1.5 mM), glucose (5 mM), and HEPES (10 mM), with the pH adjusted to 7.4. The osmolarity of this medium was 305 ± 2 mOs/kg. A low-osmolarity medium contained $MgCl_2$ (2 mM), $CaCl_2$ (1.5 mM), and HEPES (10 mM), with the pH adjusted to 7.4, and its osmolarity was 24 ± 1 mOs/kg. The hypoosmotic perfusion medium was made by mixing equal amounts of these two.

Relatively large strains were used in the experiments to minimize two possibly confounding effects: membrane potential changes and the turgor pressure of the control (preperfusion) condition. These issues are discussed in the Analysis and Discussion section. Large strains should not compromise our analysis, because a linear stress-strain relationship up to around 0.3 in length strain has been shown under voltage clamp in previous studies (Iwasa and Chadwick, 1992). Furthermore, when OHCs that were exposed to the hypoosmotic medium for up to 10 min were reexposed to the regular saline, slow recovery of their lengths was observed. For these reasons it is unlikely that irreversible damage was caused by our hypoosmotic perfusion.

Pressure release

One of the critical steps in the experiment is pressure release, which must be significantly faster than relaxation processes of the cell. Making a small hole in the membrane is the simplest and most reliable method of achieving this. After a period of hypoosmotic perfusion, cells were touched with a patch pipette to break the cell membrane and nullify the pressure difference across the membrane. The cell puncture was in every case a clear event—the pressure was released suddenly, and its length abruptly increased (see Fig. 1), although the hole was always too small to be visible. Within approximately 10 s the optical contrast of the cell was noticeably reduced with respect to the background, suggesting that the contents could flow freely out of the cell. Cells in this condition did not respond to hypoosmotic perfusion. For these reasons we believe the cells were always punctured once and could not reseal. (We have also observed in previous patch-clamp experiments that resealing is very difficult to achieve with OHCs.) After a long time (perhaps 15 min, much longer than any of the data reporter here), cells slowly lengthened to near their preperfusion lengths.

In most cases, to break the membrane, we applied a series of short (approx. 0.5 s) pulses of suction (approx. 100 Torr below atmospheric pressure) using a solenoid valve. On a number of occasions, however, cell membranes broke without being touched at all, generally near the beginning of perfusion, when stress is at a maximum. As stated above, the maximum strain encountered by cells, although large, was within the limits of a linear stress-strain curve found in earlier experiments (Iwasa and Chadwick, 1992), suggesting that "self-puncturing" cells were not stressed to structural limits overall, but simply locally at the weakest point.

Length measurement

Images of the cells during experiments were captured with a video camera and recorded with a video recorder for later analysis. Cell lengths were determined from digitized video records using the program NIH Image (Wayne Rasband, National Institutes of Health). Length strain was defined as fractional length change, $(L_0 - L)/L_0$, where L is the length at any time, and the reference length L_0 is taken before perfusion. Thus, shortening was defined as positive strain, the reverse of the standard definition. Cells with slightly curved outlines were measured with two or three line segments along their axes. The kinetics in Fig. 1 and the strain data in Figs. 2 and 3 were fit using the nonlinear Levenberg-Marquardt routine in the program KaleidaGraph (Synergy Software, Reading, PA).

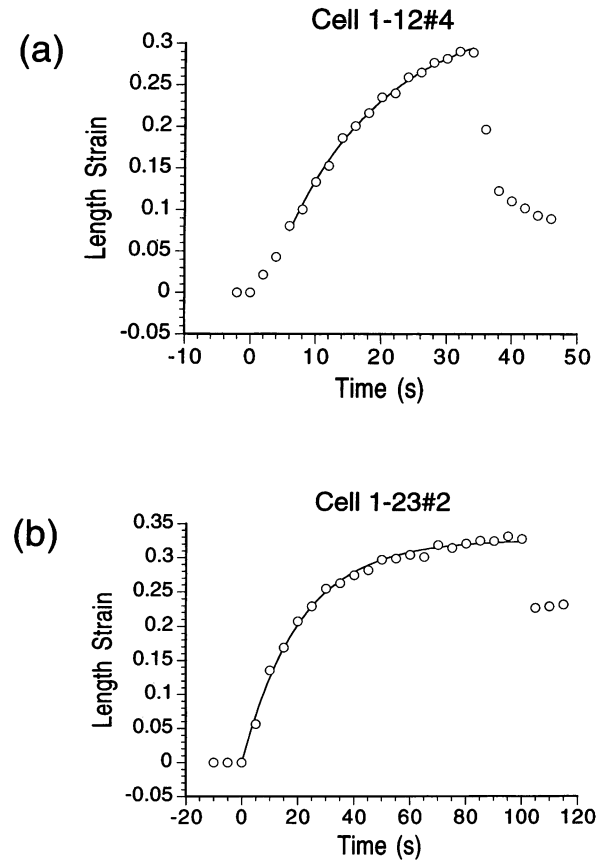

FIGURE 1 Strain kinetics. Curves are exponential fits. Length strain is defined so that cell shortening is a positive strain (see Materials and Methods). Perfusion starts at $t = 0$, and the pressure is released by puncturing the cell membrane at a later time, indicated by the drop in strain. The strain recovery "tail" after puncture in *a* results from the finite time of water exit through the hole in the cell membrane; the schematic in Fig. 4 shows such recoveries as instantaneous. In *a* the 36-s perfusion time leads to a release strain of 0.08, and the time constant is 15 s. In *b* the 102-s perfusion time leads to a release strain of 0.23, and the time constant is 21 s. The fits allowed an additional free parameter for a time offset, because the exponential time course took a few seconds to be established, in some cases. In *a* the offset is 2 s, and in *b* it is 0.1 s. Nonzero release strains indicate that the system has nonelastic components, so it must be described with a viscoelastic theory.

RESULTS

The cells did not undergo significant shape changes for at least 20 min in the standard external medium. When perfused with the hypoosmotic medium, the cells swelled, decreasing in length and increasing in diameter simultaneously. (Volume increased because the diameter increase more then compensated for the length decrease.) Fig. 1 shows strain kinetics with exponential fits for two cells for which the time constants are 15 s and 21 s. In Fig. 2 the length strain immediately before pressure release, which we

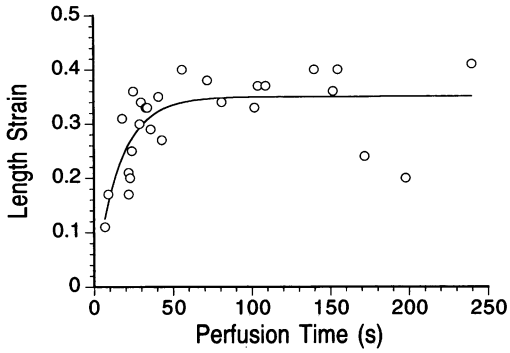

FIGURE 2 Prerelease strain. The prerelease length strain is the strain immediately before pressure release and is plotted against perfusion time for each of the 27 cells examined. Perfusion time is defined as the time from the start of perfusion until the moment of cell puncture. We used these data, with one point per cell, to determine the parameters of the average time course of imposed strain, because this method is consistent with the one-point-per-cell data in Fig. 3 (see Model section). It also allows direct comparison of data from the two plots for any particular cell. The curve is a fit to an exponential (Eq. 3) and determines $\tau_0 = 16 \pm 3$ s and $\epsilon_0 = 0.35 \pm 0.02$.

call "prerelease strain", is plotted for the cells examined, and the time constant is 16 ± 3 s.

Making a small hole in the cell membrane and releasing the pressure causes an immediate elongation, which is completed within about 10 s, followed by a much slower elongation. Because this slower recovery may take place with the cell interior exposed to the bathing medium, we did not study it closely, except to note that it is slow and clearly distinguished from the fast recovery. (Only the fast recovery phase is shown in Fig. 1.)

If the perfusion time was sufficiently short (compared with 40 s), the fast recovery after pressure release brought cells close to their preperfusion lengths. In other words, the release strain (strain after pressure release) was small. This behavior is consistent with pure elasticity. If the perfusion time was longer than 3 min, cells recovered only slightly from their prerelease strains. This larger release strain after a long perfusion time is a manifestation of membrane viscoelasticity; it implies that membrane tension relaxed during perfusion.

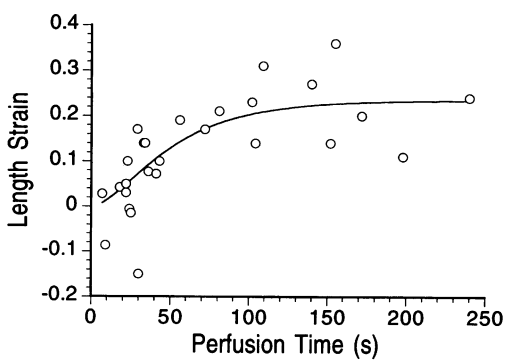

FIGURE 3 Release strain. The release strain is the strain after pressure release (allowing a short recovery time, as in Fig. 1) and is plotted against perfusion time for each cell. These data are fit to Eq. 5, holding ϵ_0 and τ_0 fixed at 0.35 and 16 s, respectively (determined from the fit in Fig. 2). The curve shows the two-parameter fit, which determines $\tau = 40 \pm 19$ s and $p = 0.5 \pm 0.2$.

The release strains for the cells examined are plotted against perfusion time in Fig. 3. Although there is some scatter in the data, showing the variability among cells, the plot shows that the release strain is significant for cells with perfusion times longer than 40 s.

Fig. 4 *a* shows a schematic of length strain versus time for two hypothetical cells with different perfusion times and indicates their expected release strains based on the model presented below. Fig. 4 *b* shows video frames of two example cells at roughly the indicated points in time.

THE MODEL

In the following, the cell is treated as a one-dimensional object for simplicity, but we show in the Appendix that a membrane theory of the cell can be reduced to the one-

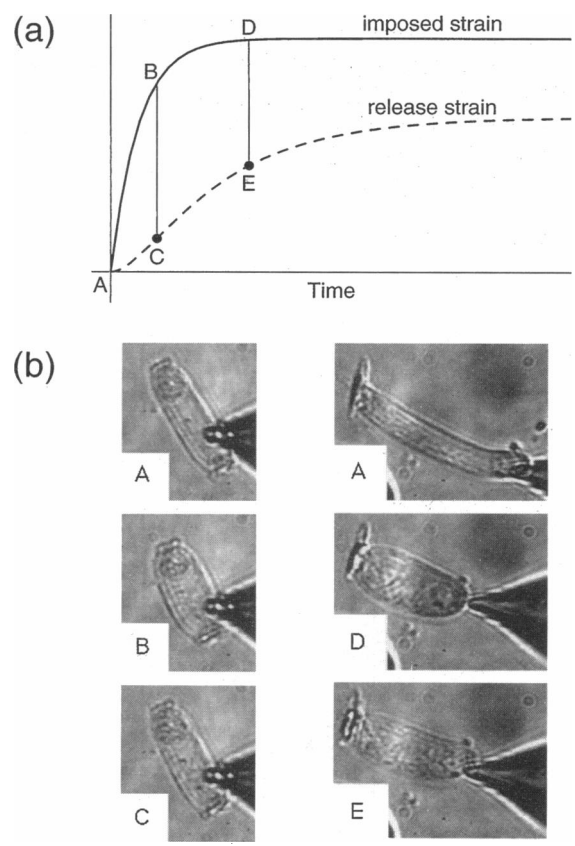

FIGURE 4 (*a*) Schematic of the experiment. Imposed strain results from the hypoosmotic perfusion, as in Fig. 1; release strain is determined from the length after puncturing the cell. (The prerelease strain plotted in Fig. 2 is the imposed strain immediately before the cell is punctured.) The schematic highlights the predicted release strains of two hypothetical cells, one with a shorter perfusion time (A→B→C) and one with a longer perfusion time (A→D→E). (*b*) The video frames show two cells at roughly the indicated points in the schematic.

dimensional description. Our experimental protocol is similar to imposing a constant strain, except for the beginning of the perfusion, when swelling takes place. The rate of the initial swelling process is primarily determined by water influx to the cell. An equilibrium is reached when the osmotic difference across the cell membrane is mostly eliminated by the increase in cell volume, and a small osmotic pressure difference is countered by a small hydrostatic pressure difference (maintained by membrane tension).

What model can explain the viscoelastic behavior as shown in Fig. 4? The data cannot be explained by either a Voigt or a Maxwell element alone (Tschoegl, 1989), because neither model has the property that the release strain is at all times different from both the prerelease strain and the equilibrium strain (Fig. 5, *a* and *b*). The simplest model that is consistent with our observations is a series connection of a spring and Voigt element (Fig. 5 *c*), called a "three-parameter Voigt model" by Tschoegl (Tschoegl, 1989; Poznański et al., 1992). It always exhibits a release strain different from the prerelease strain, and the release strain depends on the duration for which the prerelease strain is maintained.

If strain is maintained for a short time before release (compared with the characteristic relaxation time of the Voigt element), we observe only the effects of the first spring, and the system's behavior is fully elastic. After infinite time, the dashpot has no effect, and we have two springs with strains in proportion to their spring constants. The ratio k_2/k_1 (defined as p) therefore determines the extent to which the cell recovers its original length after pressure release (if stressed for a long time). In the following, we derive the functional form expected for the stress relaxation and the release strain data (Fig. 3).

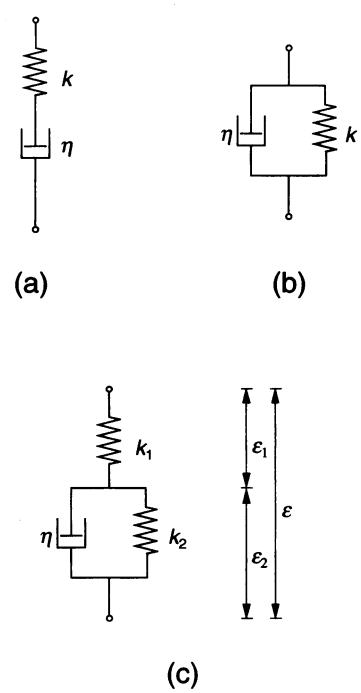

FIGURE 5 (*a*) The Maxwell element combines a spring (stiffness k) with a dashpot (viscosity η) in series. (*b*) The Voigt element combines a spring and dashpot in parallel. (*c*) Combination of a spring and a Voigt element. We use this model in the analysis. In the equations, ϵ, ϵ_1, and ϵ_2 represent strains (as in our length strain definition in the Materials and Methods section), not lengths.

The system in Fig. 5 *c* includes a spring with stiffnesses k_1 in series with a Voigt element containing a spring with stiffness k_2 and a dashpot characterized by η. The total strain ϵ is the sum of ϵ_1, the strain of the spring of stiffness k_1, and ϵ_2, the strain of the Voigt element. These are the basic equations:

$$\sigma = k_1\epsilon_1 = k_2\epsilon_2 + \eta\frac{d\epsilon_2}{dt};$$

$$\epsilon = \epsilon_1 + \epsilon_2,$$

where σ is the stress applied across the whole system, and ϵ is the total strain. Eliminating ϵ_1 and ϵ_2 we obtain this differential equation for the system:

$$\frac{d\sigma}{dt} + \frac{k_1 + k_2}{\eta}\sigma = k_1\frac{d\epsilon}{dt} + \frac{k_1k_2}{\eta}\epsilon. \quad (1)$$

Response to constant strain

For purposes of comparison, we first solve the simplest case, where a constant strain ϵ_0 is imposed on the system in a single step at $t = 0$ ($\epsilon = 0$ for $t < 0$). Under the necessary continuity condition that $\sigma(0) = k_1\epsilon_0$, we have this solution:

$$\frac{\sigma(t)}{\epsilon_0} = k' + (k_1 - k')e^{-t/\tau}, \quad (2)$$

where

$$\tau = \frac{\eta}{k_1 + k_2} \quad \text{and} \quad k' = \frac{k_1k_2}{k_1 + k_2}.$$

This result shows that initially the system behaves like spring 1 alone, and as time passes it becomes asymptotically equivalent to springs 1 and 2 connected in series. The stress and strain for this simplified case are shown schematically in the inset of Fig. 6. The response to constant strain is qualitatively similar to the case below, which is more correct, but more mathematically complicated.

Response to exponential strain

In our experiments, the strain was not applied instantaneously, but with a time dependence that was well described by an exponential function:

$$\epsilon(t) = \epsilon_0(1 - e^{-t/\tau_0}), \quad \text{for} \quad t \geq 0. \quad (3)$$

Using Eq. 1, with ϵ given by Eq. 3, and the initial

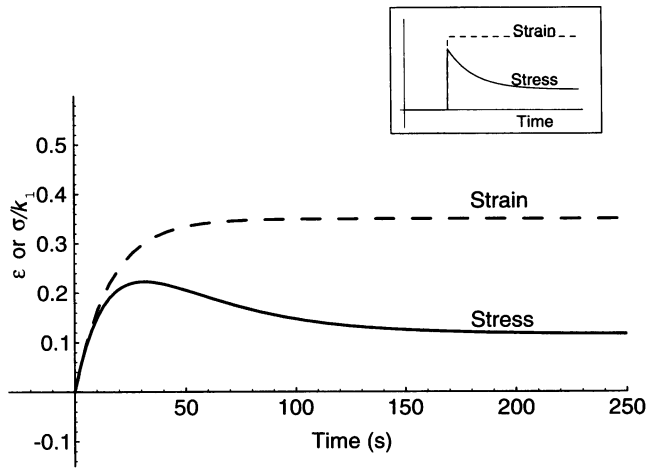

FIGURE 6 Calculated stress (see Eq. 4). The stress relaxation $\sigma(t)/k_1$ is determined from the fit in Fig. 3. The dashed line is the typical strain applied and is identical to the fit in Fig. 2. At short times, where the curves match, a purely elastic description is reasonable, with a spring constant of k_1; at long times a spring constant of $k_1k_2/(k_1 + k_2)$ is approached. The inset shows the analogous figure schematically for the case of constant applied strain (Eq. 2).

condition $\sigma(0) = 0$, we derive the stress:

$$\sigma(t) = k_1\epsilon_0\left[1 - e^{-t/\tau_0} - \frac{1}{1+p}\left(1 - \frac{\tau}{\tau - \tau_0}e^{-t/\tau} + \frac{\tau_0}{\tau - \tau_0}e^{-t/\tau_0}\right)\right], \quad (4)$$

where

$$p = \frac{k_2}{k_1} \quad \text{and} \quad \tau = \frac{\eta}{k_1 + k_2}.$$

Eq. 4 shows the time course of the stress relaxation we expect during perfusion with the hypoosmotic medium. This equation represents the main effect our experiments were designed to measure, and the function is plotted in Fig. 6, with parameters taken from the fit of release strain data in Fig. 3.

In our experiments we observed this stress relaxation by measuring the strain immediately after releasing the stress. When the cell membrane is punctured at time t_r, stress is removed instantaneously, and ϵ_1 becomes zero. The release strain ϵ_r measured at this moment consists only of ϵ_2:

$$\epsilon_r(t_r) = \epsilon_2(t_r) = \epsilon(t_r) - \frac{\sigma(t_r)}{k_1}.$$

This leads to the release strain:

$$\epsilon_r(t_r) = \frac{\epsilon_0}{1+p}\left(1 - \frac{\tau}{\tau - \tau_0}e^{-t_r/\tau} + \frac{\tau_0}{\tau - \tau_0}e^{-t_r/\tau_0}\right). \quad (5)$$

Although Eq. 5 is undefined at $\tau = \tau_0$, the function's behavior does not change as τ approaches τ_0 (the last two terms are of opposite sign, thus almost canceling each other as they become large). We present the release strain in Eq. 5 as a function of t_r, rather than t, because it only applies at a single time to a given cell. When we use this equation to fit data, we equate t_r with perfusion time, the time between the start of perfusion and the puncturing of the cell.

Of the four parameters that appear in Eq. 5, ϵ_0 and τ_0 are not related to the relaxation of stress but are determined by the time course of the swelling process alone. These parameters could be determined for individual cells. The release strain data, however, consist of one data point for each cell, so the other two parameters, p and τ, can be determined only for the ensemble of cells. For this reason, ϵ_0 and τ_0 were obtained by fitting Eq. 3 to the prerelease strain data (Fig. 2), which also consist of one point per cell. We then determined p and τ by fitting Eq. 5 (with predetermined values for ϵ_0 and τ_0) to the entire data set of release strain plotted against perfusion time (Fig. 3). Because the values for release strain are saturated with respect to time at the longest perfusion times, the spring constant ratio p is obtained relatively independently from the relaxation time τ.

ANALYSIS AND DISCUSSION

By fitting the exponential function in Eq. 3 to the prerelease strain data in Fig. 2, we obtain $\epsilon_0 = 0.35 \pm 0.02$ and $\tau_0 = 16 \pm 3$ s. With these values, the two-parameter fit of Eq. 5 to the release strain data (Fig. 3) gives $p = 0.5 \pm 0.2$ and $\tau = 40 \pm 19$ s. Although the variability among cells is appreciable in Fig. 3, the two relaxation times τ and τ_0 are reasonably well separated. We did not see a correlation between the length of the cell in the standard bath and the relaxation time.

An alternative model to the one we have used (Fig. 5 *c*) to characterize the viscoelasticity is a spring connected in parallel with a Maxwell element (Fig. 5 *a*). This network is mathematically indistinguishable from the one we have used (Tschoegl, 1989).

As a way of checking the consistency and reasonableness of our methods, we calculate the volume strain caused by an average axial strain and compare that value with the expected volume, based on knowledge of the osmotic pressure. Assuming cylindrical geometry and small strains, the relationship between volume, axial, and circumferential strains is

$$\epsilon_v = \epsilon_z + 2\epsilon_c, \quad (6)$$

where ϵ_v, ϵ_z, and ϵ_c are volume, axial, and circumferential strains, respectively. Using Eqs. 6, A1, and the last of Eq. A3, we obtain this relationship between volume and axial strains at infinite time after the imposed strain (superscript 0's indicate steady-state values):

$$\epsilon_v^0 = -\left(\frac{R+3}{R-1}\right)\epsilon_z^0,$$

where

$$R = \frac{K_1}{3\mu_1}.$$

Here, K_1 and μ_1 are elements of the area and shear moduli, respectively (see Appendix). The minus sign indicates that an increase in volume is associated with a shortening of the cell (the denominator is positive for any reasonable cell membrane). In previous work, the ratio of the two elastic moduli K/μ was measured to be about 10, based on brief pressure application under voltage clamp (Iwasa and Chadwick, 1992). In the present treatment the ratio corresponds to K_1/μ_1, because those measurements involved relatively short periods of stress to the cell. With $R = 10/3$ and $\epsilon_z^0 = -0.35$ (determined from the fit in Fig. 2, which uses the opposite sign convention), we obtain $\epsilon_v^0 = 0.95$. In other words, the estimated cell volume almost doubles when perfused with a medium of half the cell's osmolarity. This evaluation is consistent with previous observations that the cell volume response to hypoosmotic perfusion is similar to that of an ideal osmometer. This consistency implies that the cylindrical model of the cell we used is justified, even though the values of strains used were relatively large.

In the present treatment, the effects of membrane potential (Iwasa et al., 1991; Harada et al., 1993) and turgor pressure (Ratnanather et al., 1993) are ignored. The change in membrane potential at the moment of pressure release is expected to be from −70 mV to 0 mV, an effect that would decrease the cell length. But even the release of tension accompanied by this large depolarization is expected to cause a membrane potential-dependent strain of only about 0.02 (Iwasa, 1993), which is relatively small compared with our typical imposed strains. In addition, the maximum possible strain is only about 0.04, which is expected if all of the membrane motors were to change from their compact to their extended states.

The cell's natural turgor pressure is slightly above the pressure of the medium and makes the cell shorter than it would be otherwise. As a result, the strain after pressure release might be reduced somewhat. Although we did obtain negative release strain values for some cells perfused for short durations, we did not observe such behavior on average.

We can draw a number of conclusions of biological relevance from our observations. The OHC membrane behaves purely elastically when it is strained for a relatively short duration up to around 10 s. If the strain is sustained for a duration closer to τ, the cell's relaxation time (about 40 s), a significant relaxation takes place in the membrane tension (as in Fig. 6). The cell behaves purely elastically again for slow strains, for which the duration significantly exceeds τ.

In response to most of the changes associated with acoustical stimulation of the organ of Corti, the OHC should behave purely elastically. The cell's mechanical response to stimuli at acoustical frequencies, which are between 20 Hz and 20 kHz, should always be elastic. The response of the OHC to steady-state displacement of the organ of Corti during continuous acoustical stimulation (Brundin et al., 1991) that lasts about a second or less must also be elastic. The relaxation of membrane tension is insignificant in these cases, so tension changes produced by such external forces should be capable of affecting the membrane motor. For these conditions, the present result justifies previous treatments of the OHC motility, which assumed a purely elastic membrane (Iwasa, 1994, 1996).

The implications of this study for so-called slow motilities (for a review, see Dulon and Schacht, 1992) of the OHC are more complex. Slow motilities of the OHC are cell length changes observed in response to various factors, including chemicals such as neurotransmitters. For these motilities the importance of second messengers, and Ca^{2+} in particular, has been reported. For a slow motility that lasts 30 s or more, the initial increase in membrane tension will be considerably reduced by the viscoelastic relaxation we have described, reducing the modulatory effect on the cochlear mechanics. We do not, however, have direct data on whether stimuli that result in slow motility affect the relaxation time.

The viscoelasticity of the OHC may be important physiologically assuming the properties we determined for relatively large strains apply also to small strains. The viscoelasticity allows the cell to adjust to slowly changing conditions in the cochlea, such as fluctuations in osmolarity. The relaxation tends to counter the effect of external changes, keeping the membrane tension relatively constant. Because membrane tension affects the cell's motility directly (Iwasa, 1994; Kakehata and Santos-Sacchi, 1995) and indirectly (through stretch-sensitive channels that influence membrane potential; Iwasa et al., 1991; Harada et al., 1993), this mechanism prevents external factors from interfering with the cell's ability to generate force. This may be regarded as an "adaptation" mechanism of the cell motor similar to the adaptation mechanism of stereocilia (Hudspeth, 1989; Assad and Corey, 1992).

The result we obtained could be important in relating the properties of isolated cells to those of cells in vivo. It is likely that the OHC is under some stress in its position between the reticular lamina and the basilar membrane. Such mechanical constraints would be essential if the motility of this cell is to modulate basilar membrane vibrations. The membrane tension in vivo, however, may not be higher than that of isolated cells, because the viscoelastic relaxation process would tend to reduce the tension resulting from the in vivo constraints.

APPENDIX: A TWO-DIMENSIONAL TREATMENT

In the text we treated the cell as if it were a one-dimensional object, for simplicity. Because the shape of the cell is held by a membranous structure, primarily the lateral membrane, the description of mechanical properties requires a two-dimensional treatment. The cell was previously described as purely elastic (Iwasa and Chadwick, 1992). Here we extend such a treatment to include viscoelasticity of the membrane and show that the one-dimensional analysis presented in the text (Eq. 5) can be justified.

We assume the cell to be cylindrical and that the shape of the cell is determined by the mechanical properties of the lateral membrane. As in the previous analyses, this system can be described with the axial strain ϵ_z, circumferential strain ϵ_c, axial tension σ_z, and circumferential tension σ_c (Iwasa and Chadwick, 1992, 1993). We use the terms "membrane tension" and "membrane stress" interchangeably. The area strain ϵ_a, shear strain ϵ_s, area stress σ_a, and shear stress σ_s are defined by these equations:

$$\begin{cases} \epsilon_a = \epsilon_z + \epsilon_c \\ \epsilon_s = \epsilon_z - \epsilon_c \end{cases}$$

$$\begin{cases} \sigma_a = \frac{1}{2}(\sigma_z + \sigma_c) \\ \sigma_s = \frac{1}{2}(\sigma_z - \sigma_c) \end{cases}. \tag{A1}$$

A general two-dimensional strain has components of both area strain and shear strain (Evans and Skalak, 1980). With these variables, the membrane elasticity equations are

$$\begin{cases} \sigma_a = K\epsilon_a \\ \sigma_s = \mu\epsilon_s \end{cases},$$

where K is the area modulus, and μ is the shear modulus.

The introduction of viscoelasticity of the type we described in the text follows the same pattern as the one-dimensional case. Namely, the spring with modulus K is replaced by a series connection of a spring with modulus K_1 and a Voigt element, which consists of a parallel connection of a spring with modulus K_2 and a dashpot with viscosity η_a. Likewise, the spring with modulus μ is replaced by a series connection of a spring with modulus μ_1 and a Voigt element, which consists of a parallel connection of a spring with modulus μ_2 and a dashpot with viscosity η_s. The system thus has six parameters.

We consider the response of a cell when a volume strain exponential in time (as in Eq. 3) is applied to the system at $t = 0$. We consider volume strains because we are describing an osmotic response of the cell. The final volume strain, to a good approximation, is the strain that would be experienced by an ideal osmometer.

The cylindrical geometry determines the relationship between the axial and circumferential tensions and the pressure difference P across the cell membrane. A simple consideration of the force balance between the pressure and tensions for a cylinder of radius R leads to these equations for the lateral membrane (Iwasa and Chadwick, 1992):

$$\sigma_z = RP/2$$

$$\sigma_c = RP.$$

These equations indicate that $\sigma_c = 2\sigma_z$, so for area and shear stresses a relationship holds even when the pressure P changes during the course of the experiment:

$$\sigma_s = -(1/3)\sigma_a. \tag{A2}$$

We assume that area strain is proportional to volume strain; this assumption implies that shear strain is also proportional to volume strain. The meaning of this simplification becomes clearer later. With this assumption, the derivation of the stresses proceeds exactly as in the one-dimensional case, with a separate differential equation analogous to Eq. 1 applying to each of the two components, area and shear. The solutions $\sigma_a(t)$ and $\sigma_s(t)$ are therefore identical in form to Eq. 4, except that σ_a involves ϵ_a^0 K_1, K_2, p_a, and τ_a; whereas σ_s involves ϵ_s^0, μ_1, μ_2, p_s, and τ_s. (ϵ_a^0 and ϵ_s^0 are the amplitudes of applied area and shear strains, respectively.)

Combining those results with Eq. A2, which gives the relationship between the stresses, we find these relationships between area and shear parameters:

$$\frac{K_2}{K_1} = \frac{\mu_2}{\mu_1} \equiv p,$$

$$\tau_a = \tau_s \equiv \tau,$$

and

$$\epsilon_s^0 = -\frac{K_1}{3\mu_1}\epsilon_a^0, \tag{A3}$$

where we have defined the two characteristic constants p and τ, which are common to the stresses in the two directions.

If the stresses maintaining the strains are released and reset to zero at time t_r, the strains due to the pure spring elements instantly return to zero, leaving the Voigt elements unchanged. As in the one-dimensional case, the axial release strain ϵ_{zr} then consists only of the Voigt elements' strain (transformed to the axial direction) immediately before the release:

$$\epsilon_{zr}(t_r) = \frac{1}{2}\left(\epsilon_a(t_r) + \epsilon_s(t_r) - \frac{\sigma_a(t_r)}{K_1} - \frac{\sigma_s(t_r)}{\mu_1}\right). \tag{A4}$$

Using the two-dimensional equivalent of Eq. 4 and Eqs. A1 and A3 in Eq. A4, we obtain the axial release strain, which has the same form as Eq. 5:

$$\epsilon_{zr}(t_r) = \frac{\epsilon_z^0}{1+p}\left(1 - \frac{\tau}{\tau - \tau_0}e^{-t_r/\tau} + \frac{\tau_0}{\tau - \tau_0}e^{-t_r/\tau_0}\right). \tag{A5}$$

The agreement between Eq. A5 and Eq. 5 justifies our one-dimensional treatment of the cell.

Finally, we briefly discuss the meaning of the critical assumption that area and volume strains are proportional, which allowed the simplification. If that assumption is not made, the time course of length strain and that of the circumferential strain can be different, resulting in more than one time constant for the imposed strains during hypoosmotic perfusion. In addition, the number of viscoelastic relaxation times present could be more than one. These factors make the analysis more complex. However, our assumption is consistent with our data, from which we cannot distinguish more than one relaxation time.

Other assumptions upon which the analysis relies are that the cell is cylindrical and that the strains are small enough that linearized elasticity theory applies. A test of the former assumption is a rough calculation of the typical volume strain of our cells, and the result suggests that the error is not appreciable (see Discussion). The latter assumption is justified because an earlier study (Iwasa and Chadwick, 1992), in which brief pressure stresses were applied under voltage clamp, did not show a systematic deviation from linearity up to the range used in this study.

We thank Dr. William Brownell, Dr. Richard Chadwick, Dr. Emilios Dimitriadis, Dr. Gerald Ehrenstein, and Dr. Joseph Santos-Sacchi for comments on the manuscript.

REFERENCES

Ashmore, J. F. 1987. A fast motile response in guinea-pig outer hair cells: the molecular basis of the cochlear amplifier. *J. Physiol. (Lond.).* 388: 323–347.

Ashmore, J. F. 1994. The cellular machinery of the cochlea. *Exp. Physiol.* 79:113–134.

Assad, J. A., and D. P. Corey. 1992. An active motor model for adaptation by vertebrate hair cells. *J. Neurosci.* 12:3291–3309.

Brownell, W., C. Bader, D. Bertrand, and Y. Ribaupierre. 1985. Evoked mechanical responses of isolated outer hair cells. *Science.* 227:194–196.

Brundin, L., Å. Flock, S. M. Khanna, and M. Ulfendahl. 1991. Frequency-specific position shift in the guinea pig organ of Corti. *Neurosci. Lett.* 128:77–88.

Dallos, P., B. N. Evans, and R. Hallworth. 1991. Nature of the motor element in electrokinetic shape changes of cochlear outer hair cells. *Nature.* 350:155–157.

Dallos, P., R. Hallworth, and B. N. Evans. 1993. Theory of electrically driven shape changes of cochlear outer hair cells. *J. Neurophysiol.* 70:299–323.

De Boer, E. 1991. Auditory physics. Physical principles in hearing theory III. *Phys. Rep.* 203:125–231.

Dulon, D., and J. Schacht. 1992. Motility of cochlear outer hair cell. *Am. J. Otol.* 13:108–112.

Evans, E. A., and R. Skalak. 1980. Mechanics and Thermodynamics of Biomembranes. CRC Press, Boca Raton, FL. 6–30, 129–141, 203–220.

Gale, J. E., and J. F. Ashmore. 1995. Non-linear capacitance in isolated patches of the lateral membrane of cochlear outer hair cells. *Biophys. J.* 68:A392.

Harada, N., A. Ernst, and H. P. Zenner. 1993. Hyposmotic activation hyperpolarizes outer hair cells of guinea pig cochlea. *Brain Res.* 614: 205–211.

Hochmuth, R. M. 1993. Measuring the mechanical properties of individual human blood cells. *J. Biochem. Eng.* 115:515–519.

Holley, M. C., and J. F. Ashmore. 1988. On the mechanism of a high-frequency force generator in outer hair cells isolated from the guinea pig cochlea. *Proc. R. Soc. Lond. B.* 232:413–429.

Huang, G., and J. Santos-Sacchi. 1993. Mapping the distribution of the outer hair cell motility voltage sensor by electrical amputation. *Biophys. J.* 65:2228–2236.

Hudspeth, A. J. 1989. How the ear's works work. *Nature.* 341:397–404.

Iwasa, K. H. 1993. Effect of stress on the membrane capacitance of the auditory outer hair cell. *Biophys. J.* 65:492–498.

Iwasa, K. H. 1994. A membrane model for the fast motility of the outer hair cell. *J. Acoust. Soc. Am.* 96:2216–2224.

Iwasa, K. H. 1996. Membrane motors in the outer hair cell of the mammalian cochlea. *Comments. Theor. Biol.* In press.

Iwasa, K. H., and R. S. Chadwick. 1992. Elasticity and active force generation of cochlear outer hair cells. *J. Acoust. Soc. Am.* 92: 3169–3173.

Iwasa, K. H., and R. S. Chadwick. 1993. Factors influencing the length change of an auditory hair cell in a tight-fitting capillary. *J. Acoust. Soc. Am.* 94:1156–1159.

Iwasa, K. H., and B. Kachar. 1989. Fast in vitro movement of outer hair cells in an external electric field: effect of digitonin, a membrane permeabilzing agent. *Hear. Res.* 40:247–254.

Iwasa, K. H., M. Li, and M. Jia. 1995. Can membrane proteins drive a cell? *Biophys. J.* 68:214s.

Iwasa, K. H., M. Li, M. Jia, and B. Kachar. 1991. Stretch sensitivity of the lateral wall of the auditory outer hair cell. *Neurosci. Lett.* 133:171–174.

Kachar, K., E. B. Brownell, R. Altschuler, and J. Fex. 1986. Electrokinetic shape changes of cochlear outer hair cells. *Nature.* 322:365–367.

Kakehata, S., and J. Santos-Sacchi. 1995. Membrane tension directly shifts voltage dependence of outer hair cell motility and associated gating charge. *Biophys. J.* 68:2190–2197.

Kalinec, E., M. C. Holley, K. H. Iwasa, D. J. Lim, and B. Kachar. 1992. A membrane-based force generation mechanism in auditory sensory cells. *Proc. Natl. Acad. Sci. USA.* 89:8671–8675.

Lieberman, M. C., and L. W. Dodds. 1984. Single neuron labeling and chronic cochlear pathology. III. Stereocilia damage and alterations of threshold tuning curves. *Hear. Res.* 16:55–74.

Poznański, J., P. Pawłowski, and M. Fikus. 1992. Bioelectrorheological model of the cell. 3. Viscoelastic shear deformation of the membrane. *Biophys. J.* 61:612–620.

Ratnanather, T., W. E. Brownell, and A. S. Popel. 1993. Mechanical properties of the outer hair cell. *In* Biophysics of Hair Cell Sensory Systems. World Scientific, Singapore. 199–206.

Santos-Sacchi, J. 1993. Harmonics of outer hair cell motility. *Biophys. J.* 65:2217–2227.

Santos-Sacchi, J., and J. P. Dilger. 1988. Whole cell currents and mechanical responses of isolated outer hair cells. *Hear. Res.* 35:143–150.

Sung, K.-L. P., and S. Chien. 1992. Influence of temperature on rheology of human erythrocytes. *Chin. J. Physiol.* 35:81–94.

Tolomeo, J. A., and C. R. Steele. 1995. Orthotropic piezoelectric properties of the cochlear outer hair cell wall. *J. Acoust. Soc. Am.* 97:3006–3011.

Tschoegl, N. W. 1989. The Phenomenological Theory of Linear Viscoelastic Behavior. Springer-Verlag, Berlin. 41–51, 80–93.